Future projects on atmospheric neutrinos

T. Tabarelli de Fatis[a]

[a]Istituto Nazionale di Fisica Nucleare, Sezione di Milano
Piazza della Scienza 3, I-20126 Milano, Italy

New results from Super-Kamiokande, K2K and SNO not only have spurred on the interest in neutrino oscillation physics, but also have started to shift the interest from discovery to precision measurements. Future projects focusing on atmospheric neutrinos are reviewed in this context. Important contributions could be made in the precision determination of the oscillation parameters, in the observation of matter effects and in the determination of the neutrino mass hierarchy. Unfortunately, the probability that the projects discussed in this review will be running in the next ten years is rather small. The only project with a shorter time scale has not been funded.

1. Introduction

The growing evidence of oscillation in atmospheric [1,2] and solar [3,4] neutrino experiments, corroborated by the first long base-line accelerator experiment [5], is shifting the interest in neutrino physics from discovery to stoichiometry, i.e. precision measurements of neutrino masses and mixings.

A pure $\nu_\mu \to \nu_\tau$ oscillation economically describes all current observations of atmospheric neutrinos. In this context, future projects on atmospheric neutrinos could significantly improve the precision on the oscillation parameters through the explicit observation of the as-yet elusive oscillation pattern in the L/E spectrum[1] of atmospheric muon neutrinos. This would also provide a direct proof of oscillations.

The three neutrino scenario, needed to fit simultaneously atmospheric and solar neutrino data, is even less constrained. In particular, a sub-dominant contribution of ν_e to atmospheric neutrino oscillations, related to a non vanishing value of the mixing angle θ_{13}, is not excluded by data [2,7]. The $\nu_\mu \to \nu_e$ transition probability could be sizeable amplified in particular regions of the spectrum through earth-induced matter effects. Depending on the sign of Δm^2, these effects occur either for neutrinos or for anti-neutrinos only. The study of earth-induced matter effects is thus a topic of major interest for future projects on atmospheric neutrinos, since it provides an handle to measure or constrain θ_{13} and to determine the neutrino mass hierarchy.

More complex scenarios, e.g. with additional (sterile) neutrino, would be needed to accommodate also the LSND results [6]. These will not be covered by the present review. Still, one should be open to unexpected results in future and more precise experiments.

[1] L and E are neutrino baseline and its energy

2. The atmospheric neutrino beam

Atmospheric neutrinos are characterized by a wide L/E spectrum (from about 1 km/GeV to 10^5 km/GeV). This not only give access to a very large range of oscillation parameters down to small Δm^2, but is also crucial to constrain non L/E contributions to the transition probability [8], expected from sub-dominant effects, like matter effects or non standard interactions.

Moreover, the very long base-lines available with atmospheric neutrinos offer the possibility to search for earth-induced matter effects. In that endeavour, atmospheric neutrino experiments are not contested by current accelerator beam programs, whose base-lines (250÷730 km) are too short for a significant effect.

Above about 1 GeV of neutrino energy, the flux of atmospheric neutrinos is up/down symmetric at the 1% level [9]. This is an ideal condition for

disappearance experiments and gives the opportunity to perform oscillation studies with little systematic uncertainties from the knowledge of the beam spectrum: down-going neutrinos constitute a *near* reference source to which compare the *far* source of up-going neutrinos.

The atmospheric neutrino beam has an approximately equal content of neutrinos and antineutrinos, which is useful for matter effect studies, if the events can be charge-classified. On the other hand, although the ratio of the ν_e to ν_μ flavours is known with reasonable approximation [9], the almost democratic flavour composition of the beam is not ideal for appearance experiments.

Due to the low intensity of the atmospheric neutrino flux, the main limitation of atmospheric neutrino experiments stems from the limited statistics, in particular at high energies. Decisive progresses require massive detectors.

3. Future atmospheric neutrino detectors

The reference against which future progress should be evaluated is given by the (not yet final) results of Super-Kamiokande, a 50 kt (23 kt fiducial) water Cherenkov detector, that is expected to run still for several years.

3.1. Water Cherenkov detectors

Some of the atmospheric neutrino measurements are limited by the available statistics, in particular of high energy neutrino events, and could be improved by extending the Super-Kamiokande concept to a larger detector mass.

A 650 kt (450 kt fiducial) Water Cherenkov detector, tentatively called UNO has been proposed [10]. In addition to atmospheric neutrinos, this detector is intended to also address the search of nucleon decay, the detection of solar and supernova neutrinos and the detection of neutrinos from long base-line beams. The UNO detector would consist of three cubic compartments of $60 \times 50 \times 60$ m^3 (Fig.1). The central compartment would be equipped with photo-multiplier with the same coverage as in Super-Kamiokande, to be fully sensitive also to low energy events (in the 10 MeV range). A less dense photo-multiplier coverage is foreseen for the two outer compartments, dedicated to high energy events.

Figure 1. The UNO detector concept.

A similar project (Hyper-Kamiokande) is discussed in Japan as candidate successor of Super-Kamiokande. It would be a 1 Mt (800 kt fiducial) water Cherenkov detector, made of eight cubic compartments of $50 \times 50 \times 50$ m^3, aligned along the JHF2K beam direction. The photo-multiplier coverage and design are still under study [11].

Water Cherenkov detectors rely on an experimental technique extensively tested by Super-Kamiokande and, to a large extent, on known technologies. Moreover, the detector is relatively cheap (around 0.5 MEuro/kt, with an additional 0.5 MEuro/kt for excavation costs). Some drawbacks are the time scale for their realization, which spans at list a decade, and the difficulty to implement a magnetic field to measure the muon charge and to extend the acceptance at high energies with semi-contained events.

On a longer times scale, a different detector concept was envisaged by the Aqua-RICH project [12]. In this approach, the use of the ring imaging technique would provide a cleaner particle identification and the measurement of the particle mo-

Figure 2. Schematic view of the MONOLITH detector. The arrangement of the magnetic field is also shown.

mentum for outgoing tracks from multiple scattering. This detector, however, still require a major R&D phase.

3.2. Magnetised Iron Neutrino Detectors

A different detector concept is represented by large magnetised iron calorimeters, which offer the advantage of the measure of the muon charge: a very crucial feature to test matter effects with atmospheric neutrinos.

Moreover, for masses comparable to Super-Kamiokande, these detectors would have a much larger acceptance to high energy muons, where the muon direction gives a better estimate of the neutrino direction. This results in a considerably improved L/E resolution and overcomes the main limitation in the sensitivity to the oscillation pattern of current atmospheric neutrino experiments.

One such detector, the approved MINOS detector at Fermilab [13], has been primarily designed as long base-line beam detector. Its limited fiducial mass (about 3.5 kt) severely limits its potential contribution to atmospheric neutrino measurements.

A different concept was proposed for MONOLITH [14], a massive tracking calorimeter with coarse structure and intense magnetic field (about 1.3 T), explicitly designed for oscillation studies with atmospheric muon neutrinos in the Gran Sasso laboratory in Italy. The detector has a large modular structure (Fig.2). One module consists in a stack of 125 horizontal 8 cm thick iron planes with a surface area of 14.5×15 m^2, interleaved with 2 cm planes of sensitive elements, which provide a two-coordinate readout with good time resolution. The total mass of the detector for two modules is about 34 kt. The unit cost of this detector (about 1 MEuro/kt) is comparable to that of large water Cherenkov detectors, excavation costs are included.

The MONOLITH project was closed by INFN in fall 2001. However, a similar detector is being considered by the INO collaboration. This detector would be located in India, where it could also possibly act as a far-end detector of a long base-line beam experiment from Japan [15].

Magnetised iron neutrino detectors with masses of order 100 kt are also candidate detectors for a future neutrino factory [16]. Their performance on atmospheric neutrinos would be similar to MONOLITH but on a longer time scale.

3.3. Liquid Argon TPC's

Liquid Argon Time Projection Chambers (LAr TPC's) are also well suited to the detection of atmospheric neutrinos. The interest of these detectors stems from their superior resolution and their possibility to flavour-classify the events. With the present technology, their cost is much higher (about 10 MEuro/kt) than for iron calorimeters or water Cherenkov detectors. The implementation of a magnetic field is also not obvious.

A 600 t LAr TPC detector is being installed by the ICARUS collaboration in the Gran Sasso laboratory [17]. A proposal to increase the mass up to 3.0 kt with additional modules has been submitted [18]. The main focus of this proposal is on the detection of the ν_τ and ν_e appearance in the CNGS beam from CERN to Gran Sasso [19] and it is reviewed in other contributions to this conference [20]. Its potential contribution to atmospheric neutrino measurements is limited by the small mass. However, for some measurements, its superior resolution could compensate the reduced statistics.

In the long term, large Liquid Argon TPC's with masses in excess of 30 kt have also been considered at the Letter of Intent level [21,22].

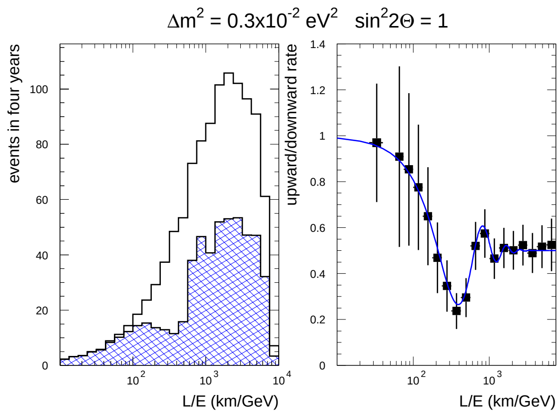

Figure 3. Left: The L/E spectrum of up-going (hatched) and the reference spectrum of down-going (open histogram) muon neutrino events. Right: Their ratio with the best-fit of ν_μ–ν_τ oscillation superimposed. Rates and errors are normalized to 4 y of MONOLITH exposure [14,24].

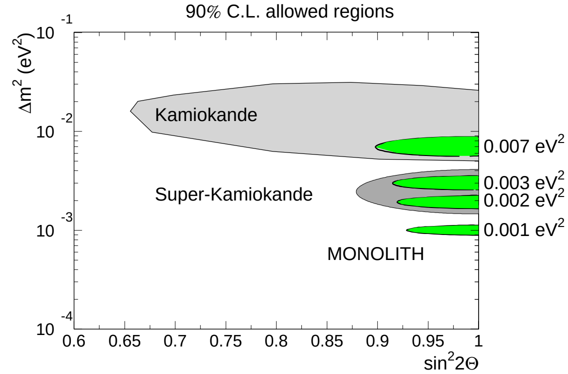

Figure 4. Expected allowed regions at 90 % C.L. for ν_μ–ν_τ oscillations after 4 y exposure. The results for $\Delta m^2 = 1, 2, 3, 7 \times 10^{-3}$ eV^2 and maximal mixing are compared to the Super-Kamiokande and Kamiokande allowed region [24].

4. Precision measurement of atmospheric ν_μ disappearance

The up/down asymmetry of high energy atmospheric muon neutrinos observed by Super-Kamiokande, gives a 10σ evidence for neutrino oscillations. This also result in a 10% precise determination of $\sin^2 2\theta_{23}$, fully dominated by the statistical error [2]. On the other hand, due to the limited L/E resolution, Super-Kamiokande does not have so far succeeded to measure an oscillation pattern in the L/E spectrum of the atmospheric muon neutrinos. Thus, a direct proof of oscillations is still outstanding and, most importantly, the measurement of Δm^2 is not accurate.

As anticipated, the much larger acceptance to high energy muons of massive magnetised iron detector, hence their improved L/E resolution, is particularly rewarding. MONOLITH, with a mass comparable to Super-Kamiokande and after a similar exposure, could already resolve the full first oscillation swing in the L/E spectrum. The expected L/E distributions of up-going neutrinos and of the reference sample of down-going neutrinos, which are assigned the baseline L they would have travelled if they were produced with a nadir angle equal to the observed zenith angle [23], are shown in Fig.3 for ν_μ–ν_τ oscillations, with $\Delta m^2 = 3 \times 10^{-3}$ eV^2 and $\sin^2 2\theta = 1.0$. In the ratio of the two distributions the oscillation behaviour is evident.

The clearness of the oscillation pattern results in a significantly improved measurement of the oscillation parameters (Fig.4), with a precision on Δm^2 and $\sin^2 2\theta$ around 6%. The observation of a first clear dip in the L/E distribution would also enable MONOLITH to disprove unconventional interpretations [25,26] of Super-Kamiokande data.

The sensitivity range for this measurement comfortably covers the entire region of parameters allowed by current results and does not strongly depend on the oscillation parameters. This is in contrast to long base-line experiments like MINOS and K2K, for which the observation of a full oscillation swing, including ν_μ "reappear-

ance", in the low Δm^2 range is not obvious.

At this level, the precision of this flux independent method is limited only by statistics. The ultimate sensitivity on the mixing angle is about 1%, due to deviations from the exact up/down symmetry of the atmospheric neutrino flux at high energy. An uncertainty of a few per cent on Δm^2 is expected from the uncertainty on the calibration of the L/E scale and on the resolution function.

Two examples of very large exposure are shown in Fig.5, where the L/E pattern expected in a Magnetised Iron Neutrino Detector (MIND) of about twice the MONOLITH mass (70 kt) and in the UNO detector (650 kt) are compared. In these detectors, higher resolution events samples could be selected, yielding an improved clearness of the L/E pattern. Due to its lower acceptance at high energies, the UNO detector needs an exposure about ten times larger then MIND to achieve the same accuracy in the reconstruction of the oscillation pattern. In other words, the plot on the right-hand side of the figure is about ten times more expensive than the plot on the left-hand side.

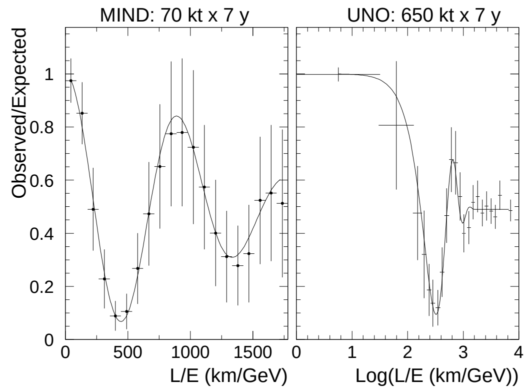

Figure 5. Expected oscillation pattern in MIND (left, adapted from Ref. [27]) and in UNO (right, adapted from Ref. [10]). Both graphs are normalised to 7 y of exposure.

5. Search for earth-induced matter effects

5.1. Matter effects from $\nu_e \rightarrow \nu_\mu$ transition at the atmospheric Δm^2

In standard three flavour scenarios, matter effects are present only for non vanishing mixing angle θ_{13}. This parameter is bound to be small by CHOOZ results [7], but the $\nu_e \rightarrow \nu_\mu$ transition can become resonant in matter and sizeably modify the oscillation probabilities of electron and muon neutrinos. An example is given in Fig.6, for $\Delta m^2 = +0.003$ eV^2 and $\sin^2 2\Theta_{13} = 0.1$, the largest valued allowed at 90% C.L. by CHOOZ. The distortions due to matter resonant transitions are particularly evident in the earth's mantle, for energies around 7 GeV and a base-line of about 9000 km. Depending on the sign of Δm^2, these effects occur either for neutrinos or for anti-neutrinos only. The sign of Δm^2, i.e. the neutrino mass hierarchy, could be determined, if the contributions of neutrinos and anti-neutrinos could be separated. The size of this effect would measure the admixture of electron neutrinos.

Since both electron an muon neutrinos are present in the atmospheric neutrino flux the transition probabilities shown in Fig.6 are not directly accessible to experiments. The observable quantity is the ratio of the observed to the expected rates of neutrino events of a given flavour, which is a combination of the conversion probabilities displayed in Fig.6, weighted by the corresponding neutrino fluxes. The observable effects are less impressive than those shown in the figure.

In ν_e appearance measurements [28], electron neutrino events can hardly be charge-classified and, in a water Cherenkov detector, only the inclusive spectrum of *e-like* events can be measured. The expectations for about 1 y of Hyper-Kamiokande exposure are shown in Fig.7, assuming $\sin^2 2\theta_{13}$ at the CHOOZ limit and positive sign of Δm^2. The resonance height would be about two times lower for negative Δm^2, since only about 1/3 of the *e-like* sample is originated by anti-neutrino interactions. The height of the resonance is also affected by the value of the mixing angle and the two quantities cannot be dis-

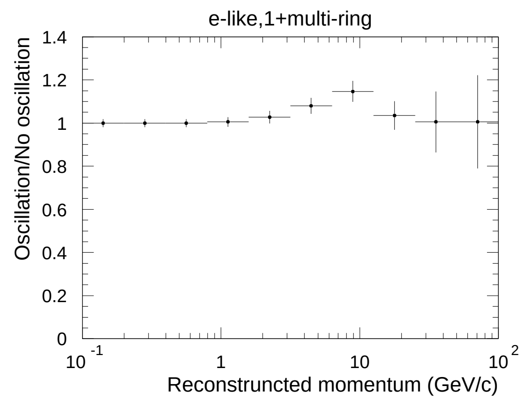

Figure 7. Ratio of up-going *e-like* events in case of three neutrino oscillation with $\sin^2 2\theta_{13} = 0.1$ to the expectations for pure $\nu_\mu \rightarrow \nu_\tau$ oscillations. Errors are normalized to an exposure of 900 kty (adapted from Ref. [28]).

Figure 6. $P(\nu_e \rightarrow \nu_\mu)$ (top) and $P(\nu_\mu \rightarrow \nu_\mu)$ (bottom) for neutrinos crossing the earth as a function of L/E and $\cos\theta_{Nadir}$. The calculation is presented for $\Delta m^2 = +0.003$ eV^2 and $\sin^2 2\theta_{13} = 0.1$. Anti-neutrinos, not shown in the figure, are not affected by matter effects for positive Δm^2.

entangled. If the mixing angle is fixed by some future long base-line experiment, the resonance height could bring information on the sign of Δm^2. With a exposure of 900 kty, the separation between $\pm\Delta m^2$ hypotheses is about at the 2σ level, for the maximum allowed value of θ_{13}.

More promising, if the value of $\sin^2 2\theta_{13}$ is not too small, seem the prospects of measuring $\sin^2 2\theta_{13}$ and the sign of Δm^2 with a magnetised iron detector, where the ν_μ disappearance can be studied separately for neutrinos and anti-neutrinos [29]. The systematic uncertainties related to the knowledge of the atmospheric neutrino rates may be controlled using the reference source of down-going neutrinos, while the electron density profile in the earth's mantle, where matter effects are observable, is known with sufficient precision. The sensitivity to $\sin^2 2\theta_{13}$ is thus limited only by the available statistics up to an exposure of about 1 Mty, corresponding to a sensitivity around 0.02 on the mixing parameter (Fig.8). Beyond that limit, resonant effects would produce spectral distortions comparable to the experimental resolution and cannot be resolved.

The range of sensitivity to $\sin^2 2\theta_{13}$ achievable with atmospheric neutrinos will be most probably covered by projects searching for the direct $\nu_\mu \rightarrow \nu_e$ transition with conventional neutrino beams, like MINOS [30], ICARUS [18] and JHF2K [11]. Even with positive evidence, however, these experiments can not measure the sign of Δm^2, which can be tested with atmospheric neutrinos by comparing neutrino to anti-neutrino spectra. The sensitivity to the sign of Δm^2 is shown in Fig.9 for MONOLITH and under different assumptions on a potential prior knowledge of $\sin^2 2\theta_{13}$. For unknown $\sin^2 2\theta_{13}$, the expected sensitivity is about two times better for positive

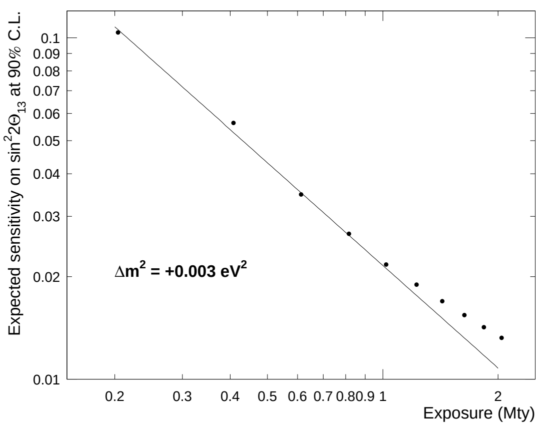

Figure 8. Expected upper limits at 90% C.L. as a function of the exposure, if no matter effects are observed in MIND. $\Delta m^2 = +0.003$ eV^2 is assumed. The line shows the scaling behaviour expected from statistical fluctuations only [29].

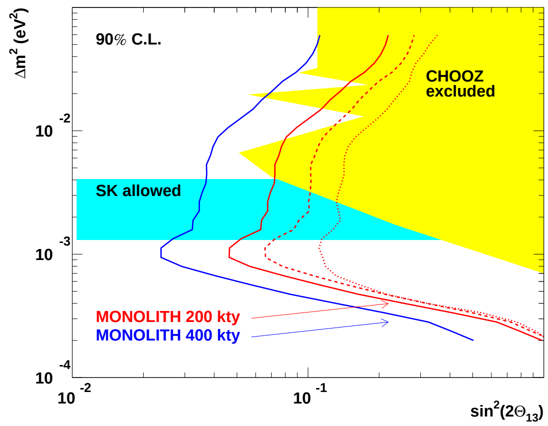

Figure 9. Regions of oscillation parameters over which the sign of Δm^2 can be determined at the 90% C.L. after MONOLITH exposures of 200 kty (6 y), assuming that $\sin^2 2\theta_{13}$ be known with 30% accuracy (full line), that $\sin^2 2\theta_{13}$ be unknown and Δm^2 positive (dashed) and that $\sin^2 2\theta_{13}$ be unknown and Δm^2 negative. The first curve is also reproduced for 400 kty. The regions excluded by CHOOZ and allowed by Super-Kamiokande at 90% C.L. data are also shown [29].

than for negative sign of Δm^2, due to the larger event rate of atmospheric neutrinos than anti-neutrinos. Assuming that $\sin^2 2\theta_{13}$ be determined with 30% precision at future accelerator experiments, an exposure of 200 kty (6 y) would be sufficient to fully evade the CHOOZ exclusion region. The sensitivity scales according to Fig.8, with an ultimate sensitivity for $\sin^2 2\theta_{13} \simeq 0.01$ at very large exposures.

On a longer time scale, a large LAr TPC with magnetic field, e.g. [22], could simultaneously test ν_e appearance and ν_μ disappearance for matter effects. This and the better energy resolution should in principle give a good sensitivity.

5.2. The LMA solution with high Δm^2_{solar}

Important distortions in the sub-GeV range of the spectrum of atmospheric electron neutrinos are predicted by the Large Mixing Angle (LMA) solution of the solar neutrino problem, provided Δm^2_{solar} is high. This scenario, that would also be affected by matter effects, has been advocated as a possible solution of the normalization problem of sub-GeV electrons in Super-Kamiokande [31,32]. For exactly maximal $\sin^2 2\theta_{23}$, the observation of such distortions would be a clean indication of a non vanishing θ_{13}.

In large water Cherenkov detectors, the effect could become statistically visible. However, the zenith angle dependence is totally smeared by the experimental resolution at low energies and a precise knowledge of the absolute normalization of the atmospheric neutrino flux would be required. This limitation might be overcome in LAr TPC's, which are sensitive also to the hadrons produced in the neutrino interactions and could reconstruct the neutrino direction with a resolution limited only by Fermi motion and nuclear effects. Still, the effects are tiny, and a decisive measurement could be made only with very large detectors.

6. Conclusions and acknowledgements

Future projects on atmospheric neutrinos could perform precision measurements of the oscillation parameters and could provide a direct proof of the oscillation mechanism through the explicit observation of the (as-yet elusive) oscillation pattern in the L/E spectrum of atmospheric muon neutrinos. The hierarchy of the neutrino mass spectrum could be determined through the observation of matter effects is a massive (magnetised) detector. The time scale for these projects is not shorter that ten years.

I am indebted to G. Battistoni, C.K. Jung, M. Shiozawa, R. Gandhi, A. Geiser, P.J. Litchfield, A. Marchionni, S. Ragazzi and many others for their help. I also thank the organizers of the Neutrino 2002 conference for their hospitality.

REFERENCES

1. Y. Fukuda et al., Super-Kamiokande Coll., Phys. Rev. Lett. 81 (1998) 1562; Phys. Rev. Lett. 82 (1999) 2644; Phys. Lett. B467 (1999) 185; Phys. Rev. Lett.85 (2000) 3999.
2. M.Shiozawa, these proceedings.
3. Y. Fukuda et al., Super-Kamiokande Coll., Phys. Lett. B 539 (2002) 179.
4. Q.R. Ahmad et al., SNO Coll., Phys. Rev. Lett. 87 (2001) 071301; Phys. Rev. Lett. 89 (2002) 011301; Phys. Rev. Lett. 89 (2002) 011302.
5. K.Nishikawa, these proceedings.
6. C. Athanassopoulos et al., LSND Coll., Phys. Rev. Lett. 81: (1998) 1774.
7. M. Apollonio et al., CHOOZ Coll., Phys. Lett. B 466 (1999) 415.
8. P. Lipari and M. Lusignoli, Phys. Rev. D60 (1999) 013003.
9. P. Lipari, T. K. Gaisser and T. Stanev, Phys. Rev. D 58 (1998) 073003;
   T. K. Gaisser, these proceedings.
10. C.K. Jung, International Workshop on Next Generation Nucleon Decay and Neutrino Detector (NNN 99), Stony Brook, New York, USA, 23-25 Sep 1999; and hep-ex/0005046
11. T. Nakaya, these prceedings;
    Y. Itow et al., hep-ex/0106019;
    T. Nagae, Nucl. Phys. A639 (1998) 551.
12. P. Antonioli et al., Nucl. Instr. Meth. A433 (1999) 104.
13. The NUMI-MINOS Project, MUNI-L-375 report, May 98; The MINOS Detectors TDR, NUMI-L-337 report, Oct 98;
    D.Michael, these proceedings.
14. N.Y. Agafonova et al., The MONOLITH Proposal, LNGS P26/2000, CERN/SPSC 2000-031, August 2000.
15. R. Gandhi, private communication.
16. A. Cervera, F. Dydak, J. Gomez Cadenas, Nucl. Instr. Meth. A451 (2000) 123.
17. ICARUS coll., LNGS - 94/99, Vol.I&II.
18. ICARUS coll., F. Arneodo et al., LNGS-EXP 13/89 add. 2/01, addendum to LNGS-94/99.
19. K. Elsener (editor), CERN 98-02 and INFN/-AE-98/05, May 1998;
    R. Bailey et al., CERN-SL-99-034-DI, June 1999.
20. S. Katsanevas, these proceedings.
21. ICARUS Coll., F. Arneodo et al., CERN/-SPSC 98-33, Oct 98.
22. D.B. Cline, F. Sergiampietri, J.G. Learned, K. McDonald, astro-ph/0105442.
23. P. Picchi and F. Pietropaolo, ICGF RAP. INT. 344/1997, Torino 1997; CERN SCAN–9710037.
24. T.Tabarelli de Fatis (for the MONOLITH coll.), Nucl. Phys. Proc. Suppl. 110 (2002) 352.
25. V. Barger et al., Phys. Lett. B 462 (1999) 109.
26. E. Lisi, A. Marrone, and D. Montanino, Phys. Rev. Lett. B 85 (2000) 1166.
27. A. Geiser, Presented at the XIX International Conference on Neutrino Physics and Astrophysics, (Neutrino 2000), Sudbury, Canada, June 2000.
28. T. Kajita, Presented at the JHF Workshop, Kamioka, Japan, May 2001.
29. T.Tabarelli de Fatis, Eur. Phys. J. C24 (2002) 43.
30. A. Para, hep-ph/0005012.
31. O.L.G. Peres and A.Yu. Smirnov, Nucl. Phys. Proc. Suppl. 110 (2002) 355.
32. M.C. Gonzalez-Garcia and M. Maltoni, hep-ph/0202218.

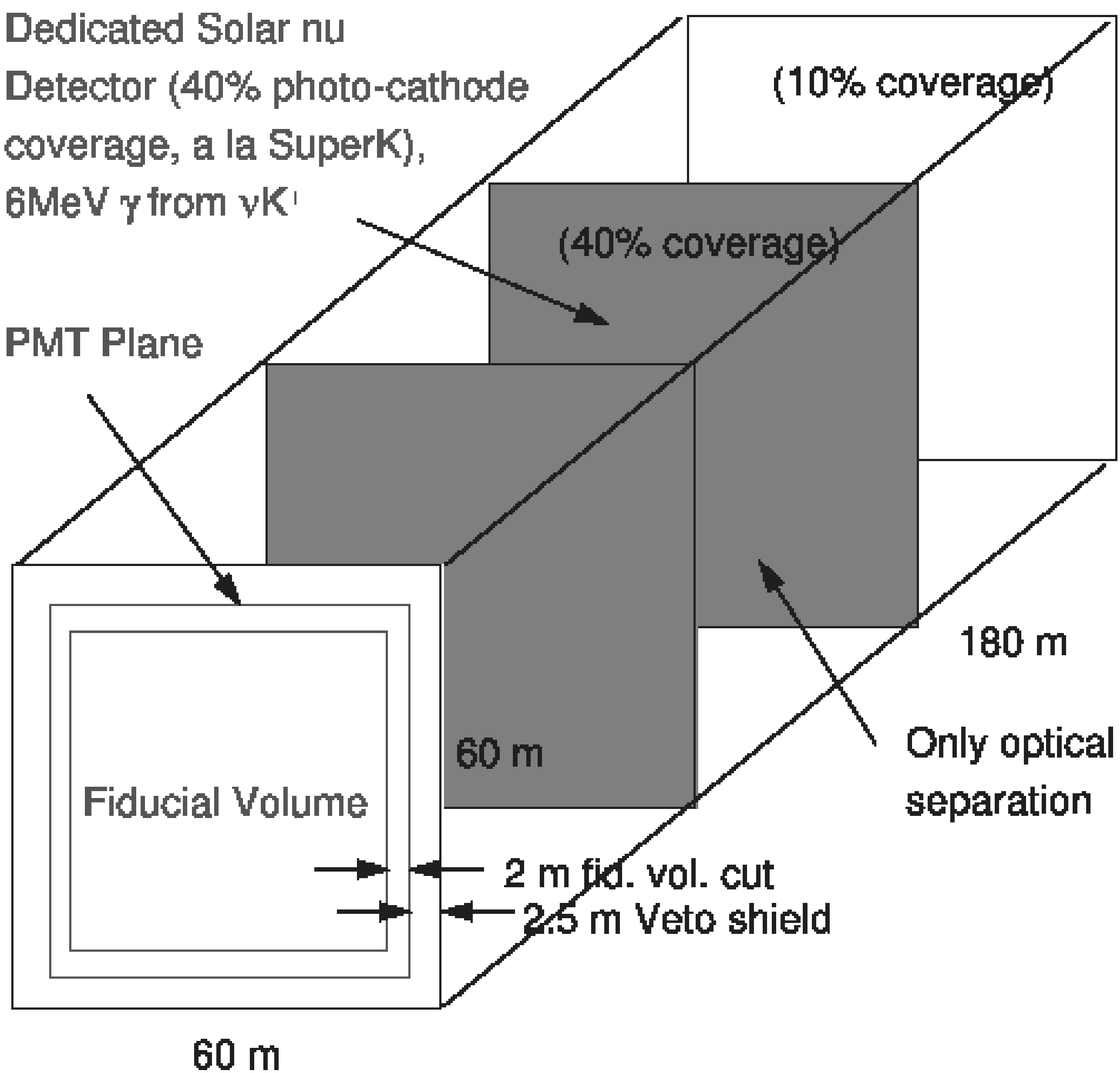

Dedicated Solar nu
Detector (40% photo-cathode
coverage, a la SuperK),
6MeV γ from νK
(10% coverage)
(40% coverage)
PMT Plane
180 m
60 m
Only optical
separation
Fiducial Volume
2 m fid. vol. cut
2.5 m Veto shield
60 m

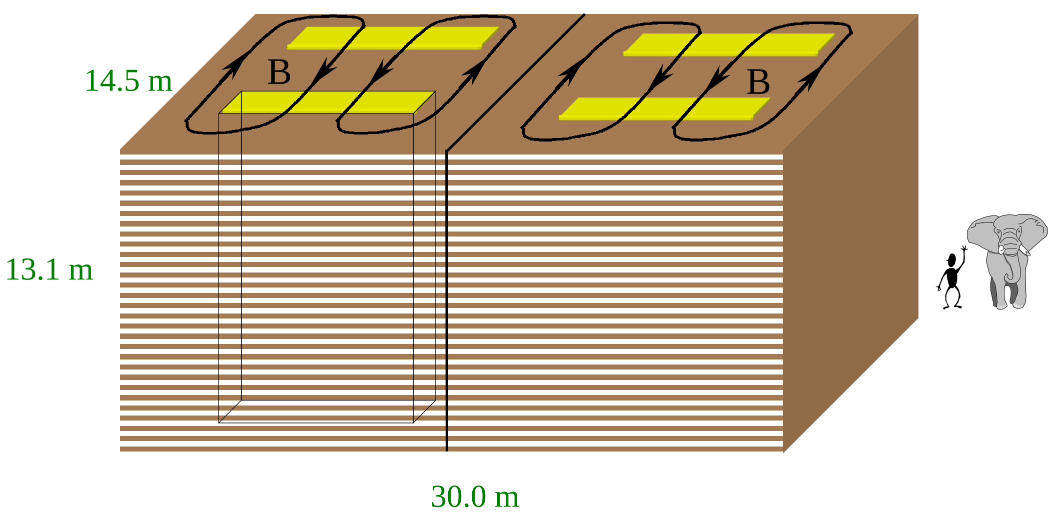

14.5 m
B
B
13.1 m
30.0 m

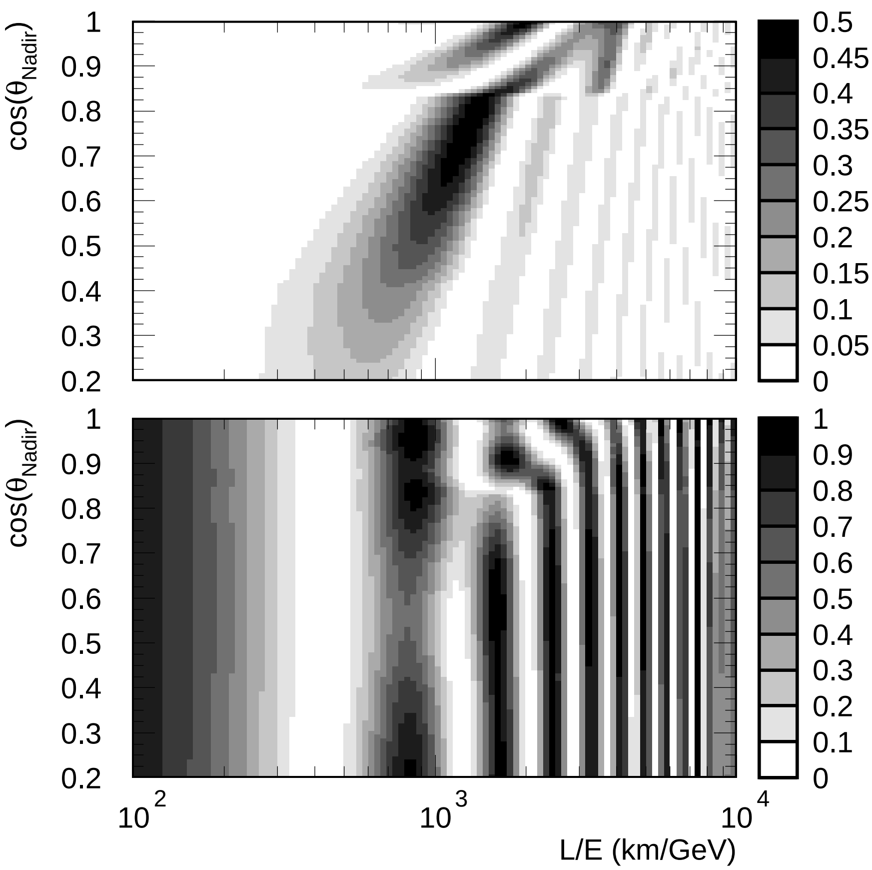

cos(θ_Nadir)
1
0.9
0.8
0.7
0.6
0.5
0.4
0.3
0.2
0.5
0.45
0.4
0.35
0.3
0.25
0.2
0.15
0.1
0.05
0
cos(θ_Nadir)
1
0.9
0.8
0.7
0.6
0.5
0.4
0.3
0.2
1
0.9
0.8
0.7
0.6
0.5
0.4
0.3
0.2
0.1
0
10^2
10^3
10^4
L/E (km/GeV)